Chem Soc Rev

View Online
Dynamic Article Links

Cite this: *Chem. Soc. Rev.*, 2011, **40**, 2279–2292

www.rsc.org/csr

TUTORIAL REVIEW

Evolution in the understanding of [Fe]-hydrogenase†

Michael J. Corr and John A. Murphy*

Received 19th October 2010
DOI: 10.1039/c0cs00150c

Published on 01 March 2011 on http://pubs.rsc.org | doi:10.1039/C0CS00150C
Downloaded by Ludwig Maximilians Universitaet Muenchen on 28 June 2011

Hydrogenases catalyse redox reactions with molecular hydrogen, either as substrate or product. The enzymes harness hydrogen as a reductant using metals that are abundant and economical, namely, nickel and iron, and should provide new pointers for the economic use of hydrogen in manmade devices. The most recently discovered and perhaps the most enigmatic of the hydrogenases is the [Fe]-hydrogenase, used by certain microorganisms in the pathway that reduces carbon dioxide to methane. Since its discovery some twenty years ago, [Fe]-hydrogenase has consistently provided structural and mechanistic surprises, often requiring complete re-evaluation of its mechanism of action. This *tutorial review* combines recent advances in X-ray crystallography and other analytical techniques, as well as in computational studies and in chemical synthesis to provide a platform for understanding this remarkable enzyme type.

Introduction

Production of 'biogas' fuel, rich in methane, is a topic of growing economic and ecological importance. The methanogen microorganisms that perform this task are archaea, and the enzymes within the archaea that take part in catalytic cycles where carbon dioxide is reduced to methane use various feedstocks as the reducing source.[1] Among these, our fascination is with the use of dihydrogen as the reducing agent. Through syntrophy,[2] different microorganisms conspire to produce and to utilise dihydrogen in the reduction of carbon dioxide. For example, the so-called *Methanobacillus omelianskii* culture[3] is a co-culture of two partner organisms, strain S and strain M.o.H.;[4] the two strains cooperate in the conversion of ethanol to acetate and carbon dioxide to methane by intimate inter-species dihydrogen transfer (Scheme 1).

The two most prevalent types of hydrogenases are known as [FeFe]-hydrogenase (containing iron–sulfur clusters) and

Strain S: $2\ EtOH + 2\ H_2O \longrightarrow 2\ AcO^{\ominus} + 2H^{\oplus} + 4\ H_2$

Strain M.o.H.: $4H_2 + CO_2 \longrightarrow CH_4 + 2H_2O$

Scheme 1 Cooperative use of H_2 by syntrophic organisms.

[NiFe]-hydrogenase (containing nickel and iron–sulfur clusters).[5–10] The [NiFe] hydrogenase family includes many different types including selenium-based [NiFeSe] hydrogenases.[1,5–10] A third type of hydrogenase was discovered in 1990 that did not contain nickel or iron–sulfur clusters.[11] This is known as the [Fe]-hydrogenase [previously known as iron–sulfur-cluster free hydrogenase or H_2-forming methylenetetrahydromethanopterin dehydrogenase (Hmd)] and is obtained from methanogenic archaea grown in nickel-limiting conditions. It catalyses the reversible reduction of N^5,N^{10}-methenyltetrahydromethanopterin ($CH{\equiv}H_4MPT^+$) **1** with H_2 to N^5,N^{10}-methylenetetrahydromethanopterin ($CH_2{=}H_4MPT$) **2** and a proton (Scheme 2) as a key step in the production of methane from CO_2 in methanogenic archaea ($\Delta G^{\circ\prime} = -5.5$ kJ mol^{-1}).[12]

The [Fe]-hydrogenase catalyses reversible stereospecific hydride transfer from H_2 to C_{14a} of $CH{\equiv}H_4MPT^+$ **1**, providing the *pro-R* methylene hydrogen in $CH_2{=}H_4MPT$ **2**.[13,14]

WestCHEM, Department of Pure and Applied Chemistry, University of Strathclyde, 295 Cathedral Street, Glasgow G1 1XL, UK. E-mail: John.Murphy@strath.ac.uk; Tel: +44 (0)141 548 2389

† Note added in proof: after submission of this review, two reviews on this type of enzyme, with different emphases, appeared.[61,62]

Michael Corr achieved his M.Sci. degree at the University of Strathclyde in Glasgow. He gained his PhD from the same university in 2010 following his studies with Prof. John Murphy on the synthesis and reactivity of superelectrophiles. He is currently working as a Postdoctoral Research Associate at the University of St Andrews.

John Murphy was born in Dublin and educated at Trinity College, Dublin (BA 1976) and the University of Cambridge (PhD 1980). He held Fellowships at the University of Alberta and the University of Oxford, before being appointed to the University of Nottingham to start his independent research. He moved to his current position as Merck-Pauson Professor of Chemistry at the University of Strathclyde in 1995. He obtained his DSc University of Strathclyde in 2002. His research interests are in reactivity in chemistry and biology and he is Director of the Glasgow Centre for Physical Organic Chemistry.

View Online

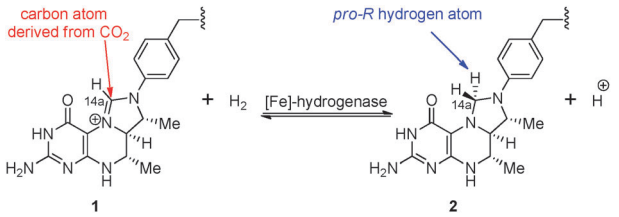

Scheme 2 Reaction catalysed by H_2-forming methylenetetrahydromethanopterin dehydrogenase, *i.e.* [Fe]-hydrogenase.

Initially, it was believed that H_2-forming methylenetetrahydromethanopterin dehydrogenase did not contain functional metal (although 1 mol iron per mol enzyme was detected at this stage),[11] making it a unique, purely organic hydrogenase.[15] This discovery led to much excitement. The proposal by Berkessel and Thauer[16] for the mechanism of action of this enzyme proved particularly interesting, as this served to extend the concept of superelectrophilic activation into the realm of enzymatic reactions, a concept that had previously been postulated only under superacid conditions. Whereas this activation may still occur in the enzymatic conversion, the enzyme was subsequently discovered to contain an iron cofactor essential for activity[17] and the enzyme crystal structure has been reported,[18,19] leading to a new range of mechanistic investigations and interest in this unusual hydrogenase. This review examines the investigations carried out on the [Fe]-hydrogenase, from its initial discovery and analysis to an assessment of the current position and prospects for the utilisation of the knowledge of its mode of action for the future.

Initial studies on H_2-forming methylenetetrahydromethanopterin dehydrogenase

5,6,7,8-Tetrahydromethanopterin (H_4MPT) **3** (Fig. 1) serves as a carrier of C_1 fragments in the metabolism of methanogenic archaea.[1] During the course of methanogenesis, a C_1 fragment is transferred to H_4MPT **3** at the oxidation level of formic acid, thereby forming **1**, which is subsequently reduced to the methyl oxidation level in a stepwise manner. During this process $CH{\equiv}H_4MPT^+$ **1** is converted to $CH_2{=}H_4MPT$ **2** by the action of a hydrogenase, then named H_2-forming methylenetetrahydromethanopterin dehydrogenase. In 1990, Thauer *et al.*[11] reported the hydrogenase activity found in *Methanobacterium thermoautotrophicum*, a thermophilic methanogen that reduces CO_2 to CH_4. The hydrogenase activity was rapidly lost under aerobic conditions or in the presence of dithiothreitol (DTT) or mercaptoethanol.[3] Hmd is

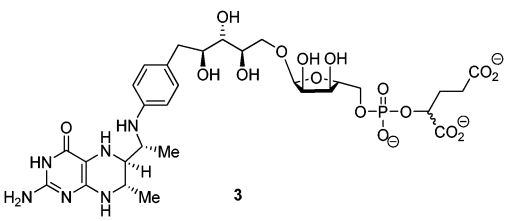

Fig. 1 5,6,7,8-Tetrahydromethanopterin **3**.

a homodimer composed of only one type of subunit that has an apparent molecular mass from SDS polyacrylamide gel electrophoresis of 43 kDa with a specific activity about 1000 U mg^{-1}.[3] Determination of the primary structure gave 37 788 Da as the actual mass of the polypeptide subunit.[20]

Both [NiFe]-hydrogenase and [FeFe]-hydrogenase mediate the reduction of viologen dyes with hydrogen.[21] In the absence of an electron–acceptor, these hydrogenases can catalyse the exchange of hydrogens between water and H_2. However, Hmd does not catalyse the reduction of viologen dyes and catalyses the exchange between H_2O and H_2 only in the presence of $CH{\equiv}H_4MPT^+$ **1** or $CH_2{=}H_4MPT$ **2**.[12] Hmd was also unusual in that it appeared to contain no functional metal.[11,12] UV-visible spectroscopy showed no absorbance above 340 nm, indicating that Hmd was not an iron–sulfur protein or flavoprotein. In addition, analysis of non-heme iron showed <0.4 mol iron per mol enzyme (in contrast with that found earlier)[11] and ICP-MS and AAS analysis showed no nickel or transition metals (levels <0.1 mol per mol enzyme).[12] The only metal found in significant quantities was zinc, found to vary between 0.5–4 mol zinc per mol enzyme depending upon the enzyme culture. However, the zinc content did not correlate with the specific activity of the enzyme.[12] The effect of CO, CN^-, acetylene, nitrite and azide as inhibitors was also investigated.[12] It was found that CO concentrations of 5% and 50% and as well as a CN^- concentration of 5% did not cause any significant loss in activity of the enzyme. Only a CN^- concentration of 50% caused a loss in activity below 50%. Nitrite, azide and acetylene were not inhibitors under the conditions of the assays.

Next, tritium exchange in the enzyme was examined.[12] When pure Hmd alone was used, no exchange between $^3H_2$ and ^1H_2O was observed at various pH values and temperatures. In the presence of $CH{\equiv}H_4MPT^+$ **1** or $CH_2{=}H_4MPT$ **2**, exchange between $^3H_2$ and ^1H_2O was observed. Using $CH{\equiv}H_4MPT^+$ **1**, isolation of the products by HPLC showed that per mol of $CH_2{=}H_4MPT$ **2** formed, 0.5 mol of ^3H was incorporated into the methylene group of $CH_2{=}H_4MPT$ **2**, consistent with transfer of a single ^3H to the substrate from the $^3H_2$ and with the release of a corresponding 0.5 mol of ^3H into the aqueous medium. Similarly using ^3H-labelled $CH_2{=}H_4MPT$ **2**, with the label distributed in the CH_2 group, the $CH{\equiv}H_4MPT^+$ formed had only half the specific radioactivity of the labelled $CH_2{=}H_4MPT$ **2**, again consistent with transfer of just one of the CH_2 hydrogens.

Various isotope studies have been conducted in order to probe the reaction between $CH{\equiv}H_4MPT^+$ **1** and dihydrogen in the presence of Hmd. Schwörer *et al.*[22] examined the production of dihydrogen from $CH_2{=}H_4MPT$ **2** using hydrogen isotopes. The purpose of these reactions was to determine if the reaction of $CH{\equiv}H_4MPT^+$ **1** with hydrogen occurred *via* hydride transfer. If this was the case, the dehydrogenation of $CD_2{=}H_4MPT$ **4** in H_2O or the dehydrogenation of $CH_2{=}H_4MPT$ **2** in D_2O would ideally produce only HD as a product, as only one of the hydrogen atoms (or deuterium atoms) could come from either substrate **2** or **4**.

The results showed that for $CD_2{=}H_4MPT$ **4** in H_2O, HD and H_2 were produced, whereas for $CH_2{=}H_4MPT$ **2** in D_2O, only HD and D_2 were produced. The production of H_2 from

Downloaded by Ludwig Maximilians Universitaet Muenchen on 28 June 2011
Published on 01 March 2011 on http://pubs.rsc.org | doi:10.1039/C0CS00150C

 This journal is © The Royal Society of Chemistry 2011

View Online

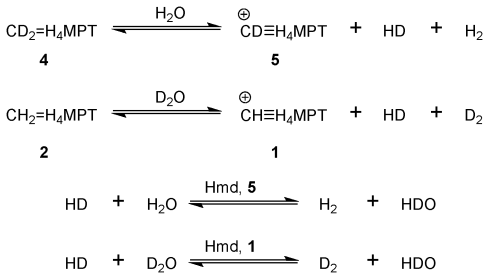

Scheme 3 Hydrogen isotope studies on the dehydrogenation of $CH_2{=}H_4MPT$ **2**.

$CD_2{=}H_4MPT$ **4** in H_2O (or D_2 from $CH_2{=}H_4MPT$ **2** in D_2O) was explained by the exchange between HD and the solvent, which was caused by $CH{\equiv}H_4MPT^+$-dependent Hmd catalysis. A summary of the reactions is shown in Scheme 3.

In the absence of $CH_2{=}H_4MPT$ **2** (or $CD_2{=}H_4MPT$ **4**), no exchange between H_2 and D_2O (or D_2 and H_2O) was observed, even when high concentrations of the enzyme were used. No generation of D_2 was observed when using $CD_2{=}H_4MPT$ **4** in H_2O and no generation of H_2 was observed when using $CH_2{=}H_4MPT$ **2** in D_2O. This indicated that only one of the hydrogens from $CH_2{=}H_4MPT$ **2** underwent reaction to form dihydrogen.

The stereochemical course of the reaction was determined by Schleucher *et al.*[13] using two-dimensional NMR spectroscopy. Reaction of $CH{\equiv}H_4MPT^+$ **1** with D_2 in D_2O led to formation of $CHD{=}H_4MPT$ **6** and $CD_2{=}H_4MPT$ **7** (Scheme 4). Formation of **6** was due to deuteride abstraction from D_2 at the C_{14a} carbon to give labelled-**6**.

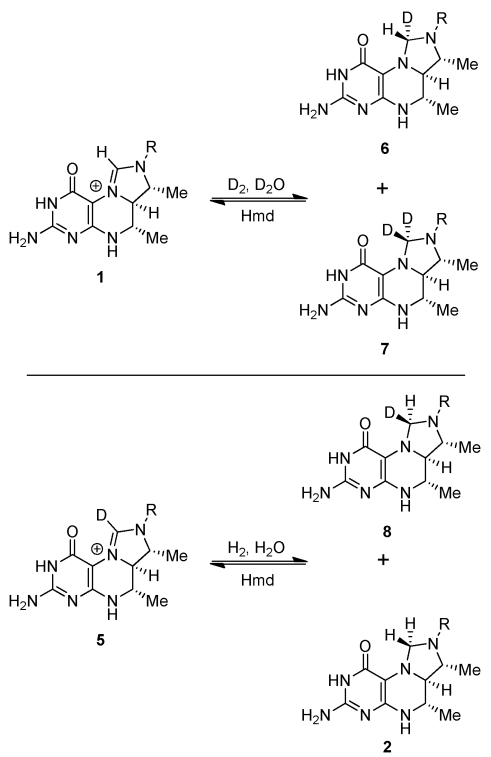

Scheme 4 NMR-labelling studies showing stereochemistry of the reaction.

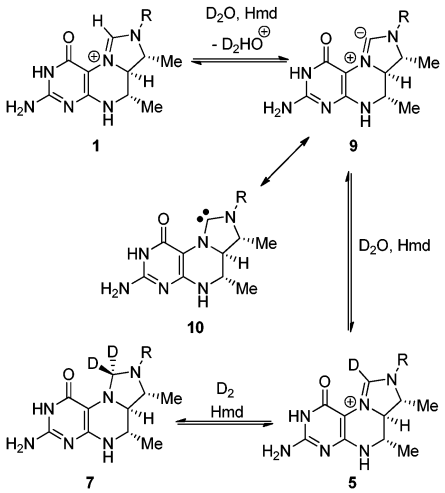

Scheme 5 H/D exchange observed in $CH{\equiv}H_4MPT^+$ **1**.

It was found that for a solution of Hmd and $CH{\equiv}H_4MPT^+$ **1** in D_2O, the signal for the methenyl hydrogen gradually disappeared, indicating exchange of the proton with D^+ from D_2O. This side-reaction was much slower than the enzyme-catalysed reaction; it was not catalysed by the enzyme and its rate increased with increasing pH. Although no discussion of its mechanism has appeared in the literature, this is most likely due to deprotonation to form **9**, which would be more usually represented as the *N*-heterocyclic carbene **10**, (Scheme 5) a reaction type more familiar in the biological chemistry of thiamine salts as well as in synthetic chemistry.[23,24] Due to this, formation of **7** in the reaction could be explained by H/D exchange of the methenyl H of **1** with D from D_2O, then reaction with D_2 to give $CD_2{=}H_4MPT$ **7** (Scheme 5). Correspondingly, reaction of $CD{\equiv}H_4MPT^+$ **5** with H_2 in H_2O led to formation of $CDH{=}H_4MPT$ **8** and $CH_2{=}H_4MPT$ **2** (Scheme 4). Determination of the absolute stereochemistry showed that hydride was transferred from hydrogen to take up the *pro-R* position of C_{14a} in $CH_2{=}H_4MPT$ **2**.

Thauer *et al.*[25] then showed the presence of a low molecular weight cofactor tightly bound to the enzyme and apparently containing no redox-active transition metal. Hmd was heterologously expressed from *Methanococcus jannaschii* and, surprisingly, showed no activity in the reduction of **1**. Hmd from *Methanothermobacter marburgensis* was denatured in urea and the ultrafiltrate (components $<$ 10 kDa molecular mass)

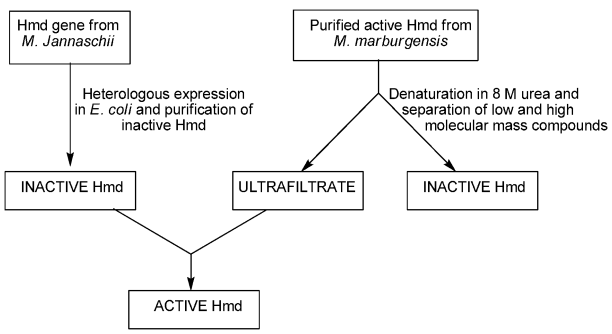

Fig. 2 Representation of Hmd ultrafiltrate reaction.

Downloaded by Ludwig Maximilians Universitaet Muenchen on 28 June 2011
Published on 01 March 2011 on http://pubs.rsc.org | doi:10.1039/C0CS00150C

View Online

Downloaded by Ludwig Maximilians Universitaet Muenchen on 28 June 2011
Published on 01 March 2011 on http://pubs.rsc.org | doi:10.1039/C0CS00150C

was collected. When the heterologously produced Hmd in *M. jannaschii* was added to the ultrafiltrate from *M. marburgensis*, the combination showed activity in the reaction of **1** with hydrogen (Fig. 2 represents the reaction performed). Similarly, Hmd heterologously expressed from *M. marburgensis* showed activity when added to the ultrafiltrate collected from *M. jannaschii*. Analysis of the ultrafiltrate showed components with a molecular mass below 1000 Da, shown, at the time, to contain no nickel and only traces of iron and zinc by TXRF analysis (Total Reflection X-ray Fluorescence spectrometry).

Superelectrophilic activation in Hmd

Although many activity studies and spectroscopic labelling studies had conclusively shown that Hmd catalysed the transfer of hydride from molecular hydrogen to CH≡H_4MPT$^+$ **1** to form CH_2=H_4MPT **2**, the mechanistic details of the reaction still remained a mystery.

In 1995, Berkessel and Thauer[16] presented an intriguing mechanistic proposal for the reaction of Hmd based on superelectrophilic activation of alkanes.[26] The proposed mechanism is shown in Schemes 6 and 7. They proposed that protonation of CH≡H_4MPT$^+$ **1** in the enzyme active site would lead to formation of superelectrophilic dicationic species **11** (or **12**). This, in turn, would increase the carbocationic character of C_{14a} in CH≡H_4MPT$^+$ **1**, allowing it to abstract hydride from molecular hydrogen to give CH_2=H_4MPT **2** (Scheme 6). This proposal was based on the work of Olah *et al.*[26–29] on the activation of alkanes for hydride exchange in the presence of superacids.

According to their proposal,[16] when CH≡H_4MPT$^+$ **1** is in the enzyme active site, it can undergo protonation on either N^5 or N^{10} to give dication species **11**/**12** (Scheme 6). Berkessel and Thauer proposed that this protonation would be accompanied by a conformational change in the imidazolinium ring to give a distorted 5-membered ring such as **14**, and that the transition state for reaction with H_2 would involve a pentacoordinated carbonium cation (Scheme 7). The antiperiplanar arrangement

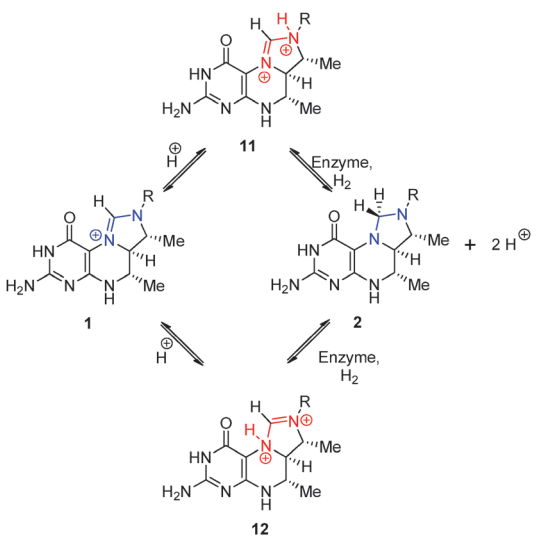

Scheme 6 Superelectrophilic activation of CH≡H_4MPT$^+$ **1**.

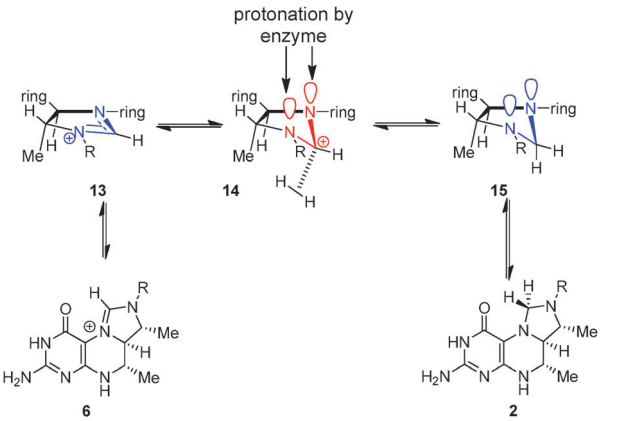

Scheme 7 Schematic representation of superelectrophilic activation in Hmd.

of the nitrogen lone pair of electrons to the C_{14a}–H bond in **14** would make it sufficiently reactive to abstract hydride from molecular hydrogen to give conformationally locked species **15**. Removal from the enzyme active site frees the nitrogen lone pair of electrons to give reduced product **2**.

Thauer *et al.*[30] later examined the rate of dihydrogen production from the reaction of CD_2=H_4MPT **4** in H_2O, based on the proposal above that the reaction occurs through a pentacoordinated carbonium cation such as **14**. Two mechanisms were proposed for the formation of H_2 in the reaction (Scheme 8).

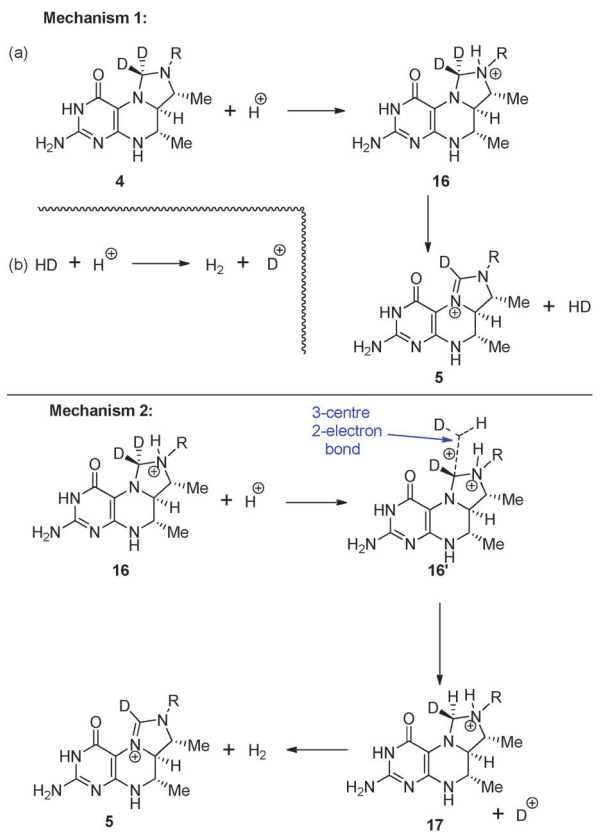

Scheme 8 Mechanisms of formation of H_2 by CD_2=H_4MPT **4**.

 This journal is © The Royal Society of Chemistry 2011

View Online

Downloaded by Ludwig Maximilians Universitaet Muenchen on 28 June 2011
Published on 01 March 2011 on http://pubs.rsc.org | doi:10.1039/C0CS00150C

In mechanism 1, protonation of $CD_2{=}H_4MPT$ **4** gives cation $[CD_2H{=}H_4MPT]^+$ **16**, which then loses HD to give $CD{\equiv}H_4MPT^+$ **5** (mechanism 1(a), Scheme 8). The HD produced can then undergo exchange with acid to give H_2 and D^+ (mechanism 1, eqn (b), Scheme 8). The second proposed mechanism again involves protonation of $CD_2{=}H_4MPT$ **4** and gives cation $[CD_2H{=}H_4MPT]^+$ **16**. Instead of loss of HD, exchange of D^+ and H^+ occurs to give onium cation $[CH_2D{=}H_4MPT]^+$ **17**, with subsequent loss of H_2 to give $CD{\equiv}H_4MPT^+$ **5**. The exchange could be envisaged as involving the transition state **16′** involving specific activation of the *pro-R* deuteron. In mechanism 1, HD is formed as an intermediate in the reaction, whereas in mechanism 2, free HD is not an intermediate in the reaction. Kinetic investigation of the mechanism could then discriminate between mechanisms 1 and 2.

They studied the kinetics of formation of H_2 and HD from $CD_2{=}H_4MPT$ **4** in H_2O and the formation of HD and D_2 from $CH_2{=}H_4MPT$ **2** in D_2O. They found that the rate of production of H_2 or D_2 was independent of the concentration of HD produced in either reaction. Based on this, the authors concluded that free H–D was unlikely to be produced in the reaction.[31] Of the two mechanisms considered, mechanism 2 was therefore preferred, in which production of H_2 or D_2 would likely occur through a transition state **16′** which undergoes stereospecific exchanges with the protons of water.

The superelectrophilic mechanism proposed by Berkessel and Thauer[16,35] precipitated a number of computational studies[32–34] on the feasibility of the reaction of amidinium ions with molecular hydrogen. However, interest in the hydrogenase was about to intensify further, thanks to an important discovery that was to be reported.[36]

From metal-free to [Fe]-hydrogenase

When Lyon *et al.*[36] reexamined the spectral properties of the Hmd hydrogenase, they made a startling discovery. They showed that Hmd was inactivated by UV-A/blue light irradiation and, from this, determined that the "metal-free" hydrogenase did in fact contain an "active" iron cofactor.

Hmd was prepared under anaerobic conditions using an anaerobic chamber filled with 95% N_2/5% H_2. These preparations showed 1 ± 0.2 mol iron per mol Hmd monomer (determined by trapping the iron in a complex with absorption maximum at 563 nm, and measuring against a $FeCl_3$ calibration curve). The Hmd stored in the dark showed no loss in activity, in contrast to samples exposed to white light, where activity decreased to zero over 30 minutes. Tests using monochromatic light showed Hmd to be inactivated by UV-A (320–400 nm) and blue light (400–500 nm). In addition, experiments showed that iron-leaching increased linearly with decrease in Hmd activity when EDTA was present and that the inactive Hmd contained no iron. When EDTA was not present, light irradiation caused bleaching and inactivation of Hmd, but almost no iron was released from the enzyme.

Shima *et al.* also re-examined the effect of CO inhibition on Hmd.[37] Previous studies[12] had shown that Hmd was not inactivated by CO concentrations of 5% or 50%. Now, however, at 100% CO concentration, Hmd activity was inhibited by over 50%. The CO concentration was ~100-fold higher than that required to inhibit most [FeFe]-hydrogenases and ~10-fold higher than for [NiFe]-hydrogenases, which was why the high level had not been previously examined. The CO inhibition was shown to be reversible, and removal of CO resulted in a return in Hmd activity.

Studies on the cofactor alone showed a light sensitivity, with the cofactor being bleached with resulting loss of iron, upon exposure to light. From these studies, Lyon *et al.*[37] proposed that Hmd contained an iron-containing cofactor (later called the FeGP cofactor, where GP is an abbreviated form of guanylylpyridinol or guanylylpyridone) that is not redox-active and is necessary for the enzyme activity. With this important discovery, the H_2-forming methylenetetrahydromethanopterin dehydrogenase could no longer be considered as a purely organic hydrogenase and a great deal of research was conducted into determining the structure of this new iron active site and its importance in the hydrogenase activity.

Light- or heat-inactivation of the cofactor released iron and CO. Chemical analysis revealed 2.4 ± 0.2 mol of CO per mol Fe in the cofactor.[38] In addition, a relatively stable product of mass 542 Da could be isolated by HPLC and analysed.[38] Structure elucidation on the stable product suggested a pyridone-type ligand consistent with **18** (Fig. 3). The pyridone structure was supported by fluorescence spectroscopy on the inactivated cofactor.

Next, Lyon *et al.*[37] examined the IR spectrum of Hmd in order to determine the ligands that were attached to the iron in the cofactor. IR analysis of the enzyme showed two absorption bands at 2011 and 1944 cm^{-1}, derived from the two intrinsic CO molecules bound to the iron atom in the cofactor. No change in the IR spectrum was observed when the enzyme's spectrum was measured under nitrogen, oxygen or hydrogen. Analysis of the intensity of the IR bands suggested the presence of an $Fe(CO)_2$ unit where the CO groups were present at an angle of 90°.

They then examined the IR spectra of CO-inhibited Hmd, CN^--inhibited Hmd and the spectrum of Hmd in the presence of **1** or **2**. Incubation of Hmd under CO led to three CO bands (2074, 2020 and 1981 cm^{-1}) of similar intensity. Incubation under ^{13}CO resulted in three bands (2050, 1999 and 1980 cm^{-1}), one of which was determined as coming from ^{13}CO. The IR spectrum reverted back to the spectrum recorded for Hmd (two CO bands at 2011 and 1944 cm^{-1}) when the gas phase was replaced with argon, H_2, N_2 or air. The authors suggested that the CO-inhibited enzyme contains three CO units and that the extrinsic CO units will not replace the two intrinsic CO molecules under any incubation times or temperatures. In addition, the extrinsic CO is readily removed upon removal of

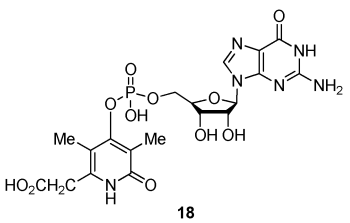

18

Fig. 3 Pyridone ligand isolated from Hmd cofactor.

View Online

Published on 01 March 2011 on http://pubs.rsc.org | doi:10.1039/C0CS00150C
Downloaded by Ludwig Maximilians Universitaet Muenchen on 28 June 2011

CO from the gas phase, but the intrinsic CO ligands are not removed.

The CN^--inhibited Hmd contained three bands at 2091, 2020 and 1956 cm^{-1}. When $^{13}CN^-$ was used as the inhibiting reagent, three bands were observed at 2047, 2017 and 1956 cm^{-1}. Based on the shifts measured, the cyanide bands were assigned to 2091 and 2047 cm^{-1} for CN^- and $^{13}CN^-$ respectively. Calculations based on the spectrum intensities indicated that the two CO units were at 90° to one another. Competition for inhibition binding between CO and CN^- showed the CN^--inhibited enzyme as the major product. This indicated that Hmd had a higher affinity for CN^- than for CO as a ligand.

Addition of **1** or **2** under the presence of argon or H_2 led to small changes in the IR spectrum of Hmd. The IR bands of the CO signals shifted slightly (from 1–7 cm^{-1}) and sharpening of the absorption bands occurred. The results suggested that **1** and **2** bind close to or at the iron site in the cofactor, resulting in a slight shift to higher frequency in the CO bands. The 20–30% decrease in the width of the absorption bands indicated less vibration of the CO positions in space, consistent with a decrease in flexibility of the active-site pocket caused by binding of **1** to the iron centre or in close proximity to it. With the addition of H_2, the effects of **1** on the IR spectrum of Hmd were amplified. This could indicate that hydrogen may directly interact with the iron centre in the presence of **1**, although the authors could find no evidence of Fe–H or Fe–D stretches in the IR spectrum.

When the iron-containing cofactor was isolated and analysed, the CO bands were found to shift from 2011 and 1944 cm^{-1} to 2031 and 1972 cm^{-1}, indicative of decreased electron density in the iron centre or a change in the total number of ligands attached.

Based on the IR analysis of the CO ligands, Lyon *et al.*[37] concluded that the iron in the Hmd cofactor was coordinated to two CO molecules. From this they concluded that the iron present in Hmd is most likely to be Fe(II); coordination to three CO molecules in the CO-inhibited Hmd makes Fe(III) unlikely, as iron(III) tricarbonyl complexes have not been reported. Fe(0) as the species is unlikely as iron(0) cyanide complexes are rare (but not unknown, $[Fe(CO)_4CN]^-$ has been reported).[39] Hmd was shown to be EPR-silent,[40] which ruled out Fe(I) as the iron species. This makes Fe(II) the most probable species to be present in Hmd, but the results did not prove the oxidation state.

In order to gain insight into the electronic structure of iron in Hmd, Shima *et al.*[40] measured the Mössbauer spectra of ^{57}Fe-labelled Hmd prepared under dark conditions. The results showed the presence of a low-spin iron in a low oxidation state. Inhibition of the enzyme by CO or CN^- showed changes in the recorded Mössbauer spectrum, an indication that the inhibitors were bound to the iron site. However, the addition of hydrogen and/or $CH{\equiv}H_4MPT^+$ **1** did not lead to any significant change in the Mössbauer spectrum. This would seem to indicate that H_2 or **1** bind near the iron in the enzyme, but are not direct ligands to the iron site, that when Hmd interacts with the substrates (H_2 and/or **1**), the electronic state of the iron doesn't change significantly.[40] This is surprising, as even if **1** does not bind to the Fe centre, it would be expected that hydrogen would need to bind to or interact with the Fe centre (and thereby to change its spectroscopic properties) in order to become activated for heterolytic cleavage.

Quantification of the Mössbauer signal intensities gave a calculated 1.14 ± 0.25 mol iron per mol protein monomer. Analysis of the magnetic properties of the three Hmd preparations (Hmd, CO-inhibited Hmd and CN^--inhibited Hmd) showed them to be diamagnetic with spin S = 0, consistent with Fe(II) or Fe(0) low-spin and not paramagnetic Fe(I) or Fe(III) low-spin. Based on the IR[41] and Mössbauer[40] studies, it appears likely that the iron present in Hmd is Fe(II). The case for an Fe(II) complex received further strong support in an infrared study of carbonyl stretch frequencies, performed by Pickett, Liu *et al.*[41] Here the enzyme and the isolated cofactor showed bands that, on comparison with known mono-iron *cis*-dicarbonyl complexes were clearly consistent only with Fe(II).

More recently, Meyer-Klaucke *et al.*[42] examined the iron-complex structure of [Fe]-hydrogenase and model systems, using X-ray absorption near-edge spectroscopy, and concluded that an Fe(II) complex was consistent with the [Fe]-hydrogenase in *M. jannaschii*.

The crystal structure revealed

In 2006, Pilak *et al.*[43] reported the crystal structure of the apoenzyme of Hmd (the enzyme without the iron-containing cofactor present) from *M. jannaschii* and *M. kandleri* at 1.75 Å and 2.4 Å resolution respectively.

Hmd from *M. jannaschii* was found to consist of a homodimer with approximate dimensions of 90 Å × 50 Å × 40 Å, subdivided into a central globular unit attached to two peripheral units in a linear manner. Each peripheral unit corresponded to the N-terminal domain of one subunit and was composed of an α/β structure that belongs to the Rossmann fold protein family (Fig. 4). The central globular unit was composed of the C-terminal segment of both subunits, each containing four α-helices that form an intertwined intersubunit helix bundle. The Hmd from *M. jannaschii* was present in a closed conformational state (Fig. 5(a)), whereas the Hmd from *M. kandleri* was found to be in an open conformational state (Fig. 5(b)). Within the crystal structure, the authors located a U-shaped electron density 13 Å long, located close to the bottom of the cleft; this is shown in green in Fig. 5 and 6. The electron density was found to be consistent with polyethyleneglycol, present in the crystallising solution. This was thought to indicate the presence of a channel for substrate delivery within the enzyme.

Activity measurements on Hmd reconstituted from *M. jannaschii* showed that for the three conserved cysteine residues (Cys10, Cys176 and Cys250), only that at Cys176 was essential for enzyme activity.[43] Based on this, Cys176 was assigned as the iron-ligating sulfur ligand.

The authors modelled the iron active site and binding of $CH_2{=}H_4MPT$ **2** in the enzyme based on the structure of the formaldehyde-activating enzyme of *M. extorquens* in a complex with $CH_2{=}H_4MPT$ **2**.[43] They found that **2** sits in the iron active site at the base of the U-shaped electron density (Fig. 5 and 6). In this position, the C_{14a} of **2** is ~6 Å from the assumed Cys176-ligated iron atom, with sufficient space for binding of molecular hydrogen. In this model, the phenyl ring

 This journal is © The Royal Society of Chemistry 2011

View Online

Downloaded by Ludwig Maximilians Universitaet Muenchen on 28 June 2011
Published on 01 March 2011 on http://pubs.rsc.org | doi:10.1039/C0CS00150C

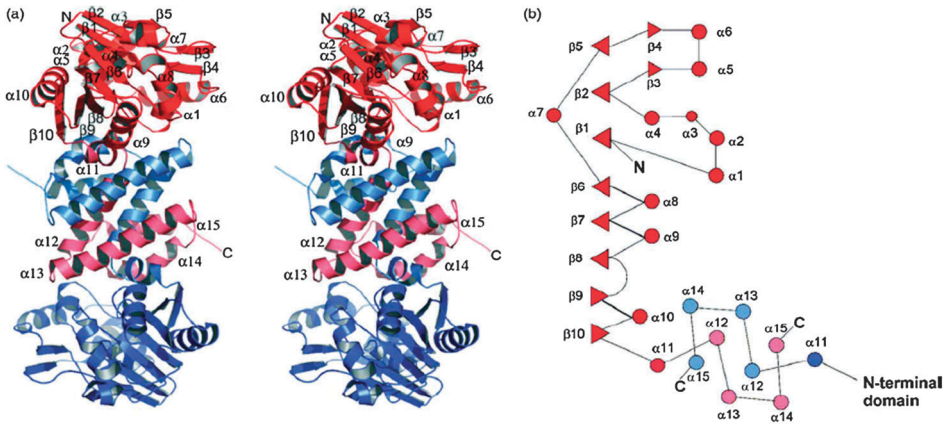

Fig. 4 Crystal structure of Hmd apoenzyme of *M. jannaschii*. Reprinted from the ref. 43, copyright 2006 with permission from Elsevier.

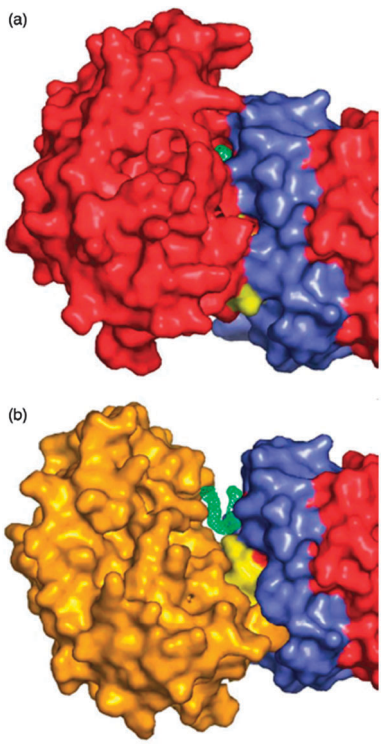

Fig. 5 (a) Closed conformational state of Hmd in *M. jannaschii*. (b) Open conformational state of Hmd in *M. kandleri*. The U-shaped electron density (see text) is shown in green. Reprinted from the ref. 43, copyright 2006 with permission from Elsevier.

Fig. 6 Model of the iron cofactor and substrate **2** in the presumed active site of Hmd in *M. jannaschii*. The model of the iron-containing cofactor is shown in yellow, the conformation of $CH_2{=}H_4MPT$ **2** taken from the crystal structure of *M. extorquens*[44] is in grey and is unchanged. Reprinted from the ref. 43, copyright 2006 with permission from Elsevier.

adjacent to the imidazolidine ring of **2** is ~4.5 Å from the pyridone ring of the cofactor ligand **18**, which the authors proposed could mean that the phenyl ring was present for binding or conformational purposes.

A later crystal structure showed that the FeGP cofactor[18] was anchored to the enzyme by a guanosine monophosphate. Within the active site, the iron atom exists in a distorted octahedron ligation shell. One of the ligands is from the nitrogen of the pyridinol ligand **19** (Fig. 7)—from X-ray analysis it is not possible to see whether the 2-substituent on the pyridine is in its protonated (hydroxy) state, or if the hydroxyl group is deprotonated. The carboxyl group in ligand **19** was disordered in the crystal structure, which led to a tentative determination of its orientation in the crystal structure. The other ligands on the iron were composed of two CO molecules at 90° to each other, consistent with previous studies,[37,40] a sulfur from the cysteine in Cys176, an unknown ligand ('U' in Fig. 7) the structure of which could not be solved due to high levels of disorder and a solvent water molecule ('O' in Fig. 7). The structure of the unknown ligand could not be determined from the electron density in the crystal structure. However, soaking the crystals in 3 mM cyanide led to a 1.6-fold increase in the electron density at this site, suggesting that it could be the site of reversible cyanide inhibition.

The ligand site *anti*- to the nitrogen of **20** was shown to contain a water molecule. However, the distance between the oxygen atom of water and the iron atom was 2.7 Å, considered too far away to be a "proper" ligand to the iron. The authors suggested that this could be the site of binding for H_2 or extrinsic CO in the CO-inhibited enzyme. The solvent molecule interacts with another solvent molecule, which in turn is linked to the carbonyl group of Cys250 (Fig. 8 and 9).

View Online

Downloaded by Ludwig Maximilians Universitaet Muenchen on 28 June 2011
Published on 01 March 2011 on http://pubs.rsc.org | doi:10.1039/C0CS00150C

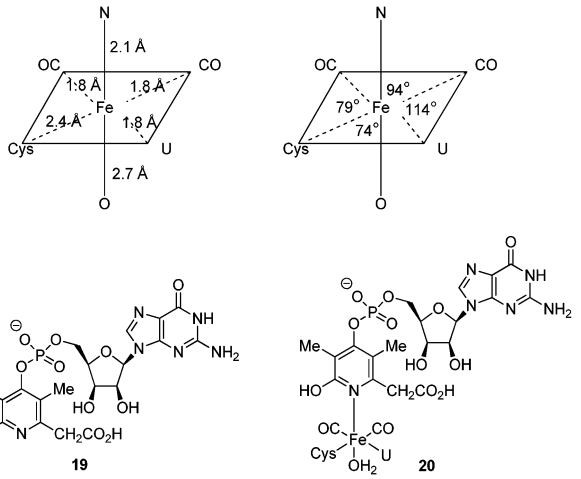

Fig. 7 Geometry of the active site of Hmd.

Shima *et al.*[18] suggested that the cleft between the peripheral and central units on the enzyme (Fig. 4) could accommodate $CH{\equiv}H_4MPT^+$ **1**, with the C_{14a} atom being positioned sufficiently close to the iron centre without distortion of the polypeptide chain. However, they stated that the inter-subunit cleft was too large for optimal $CH{\equiv}H_4MPT^+$ **1** adjustment, so that binding must be accompanied by an induced-fit movement in the enzyme.

The proposed mechanism for the reduction of $CH{\equiv}H_4MPT^+$ **1** to $CH_2{=}H_4MPT$ **2** is that the hydride accepting $CH{\equiv}H_4MPT^+$ **1** and Lewis acidic iron perform bifunctional catalysis to lower the pK_a of molecular hydrogen, allowing it to be heterolytically cleaved into hydride and a proton. Proton acceptors in the vicinity of the active site included Cys176 thiolate, the pyridinol N, O or CO and two histidines, His14 and His201. Along these lines, a His14 → Ala mutation greatly decreased the hydrogenase activity of Hmd, whereas a His201 → Ala mutation had little effect. This indicated the importance of His14 on Hmd activity, possibly as a proton acceptor in the reaction.

Based on the active site of the [Fe]-hydrogenase reported,[18] a mechanism[45] for hydride transfer to **1** and an active site model was proposed.[50] These will be discussed in the next sections of this review.

Hiromoto *et al.*[19] later revised the structure of the FeGP cofactor based on the crystal structure of a mutated Hmd enzyme. They reported the crystal structure of a holoenzyme of [Fe]-hydrogenase from *M. jannaschii* where Cys176 was

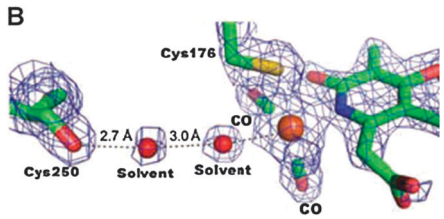

Fig. 9 Solvent interaction in the iron active site of Hmd. From ref. 18. Reprinted with permission from *AAAS*.

mutated to alanine, and in the presence of dithiothreitol (DTT) **21**, at a resolution of 1.95 Å. Significant changes were observed in the iron ligands of the FeGP cofactor that had implications for the structure of the "wild-type" enzyme previously reported.[18] When DTT **21** was present, it displaced the binding of the sulfur of Cys176 and the unknown ligand with the 1S and 2-hydroxyl O atoms of DTT **21** (Fig. 10 and 11). More significantly, the pyridinol ligand **19** was found not only to bind to the iron through the ring nitrogen, but also through the acyl carbon of the "carboxylate" group. This resulted in a 180° rotation of the pyridinol ligand from the previously determined structure **20** (Fig. 7). As a result of this new acyl binding, the second intrinsic CO ligand is repositioned to the site previously occupied by a solvent molecule. ATR-IR

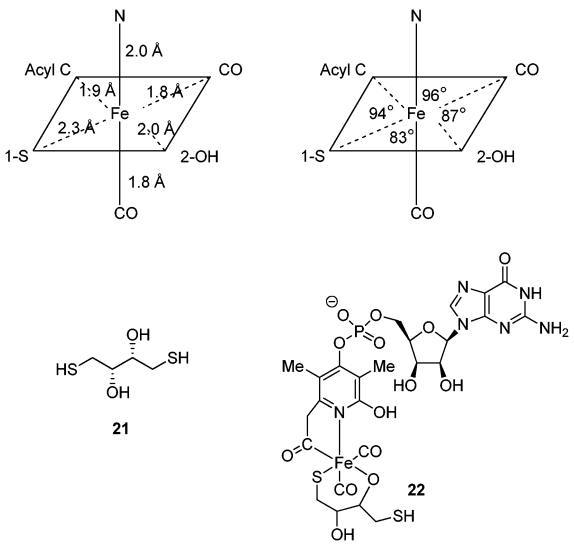

Fig. 10 FeGP cofactor geometry based on crystal structure of Cys176-Ala mutated Hmd.

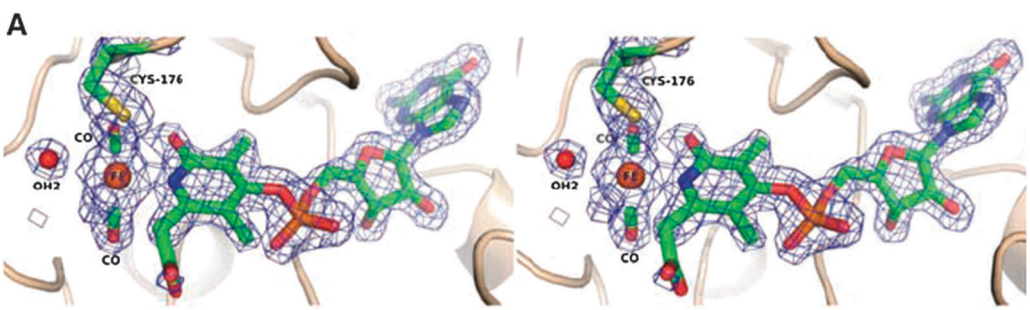

Fig. 8 Stereoview of electron density in Hmd crystal structure. From ref. 18. Reprinted with permission from *AAAS*.

 This journal is © The Royal Society of Chemistry 2011

View Online

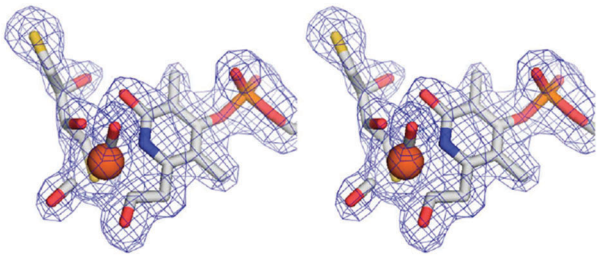

Fig. 11 Stereoview of electron density in mutated Hmd (Cys176-Ala) crystal structure. Reprinted from ref. 19, copyright 2009 with permission from Elsevier.

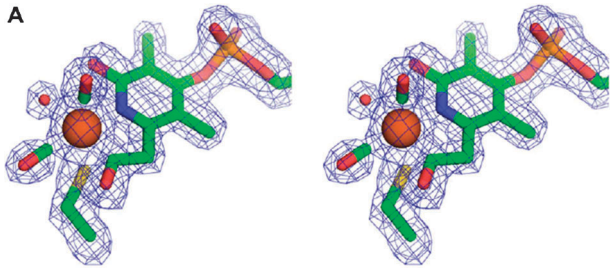

Fig. 13 Reinterpretation (stereoview) of iron-ligation structure in [Fe]-hydrogenase. Reprinted from ref. 19, copyright 2009 with permission from Elsevier.

Downloaded by Ludwig Maximilians Universitaet Muenchen on 28 June 2011
Published on 01 March 2011 on http://pubs.rsc.org | doi:10.1039/C0CS00150C

analysis of the mutated enzyme before and after the crystal structure determination still showed the presence of two CO ligands with a calculated angle of 90° between them.[46,47]

In the mutated enzyme, the hydroxyl group on the pyridinol ligand now interacted *via* a hydrogen bond to the imidazole group of His14. In addition, the oxygen of the acyl group of the pyridinol ligand was linked *via* a hydrogen bond to the amide group of Ala176.

Based on this new geometry, Hiromoto *et al.*[19] reexamined the previously reported[18] EXAFS data on the "wild-type" Hmd enzyme. Modifying the iron ligation to include the newly proposed bidentate ligation by the pyridinol ligand led to a better data fit upon re-refining. The authors stated that the "previous interpretation of the electron density was biased by the lack of imagination concerning the possibility of an acyl group as iron ligand and on the subsequent conclusion that the orientation of a negatively charged carboxylate group towards the rather unpolar protein interior is unlikely".[19] As a result of this, a new structure for the FeGP cofactor was proposed (Fig. 12 and 13). In this new structure, the authors state that the most probable site of the second intrinsic CO is that previously occupied by a solvent water molecule (Fig. 7). This was based on the crystal structure obtained for the Cys176-Ala mutated Hmd enzyme, but its position could not be identified on a structural basis from analysis of the crystal structure of the "wild-type" Hmd enzyme.

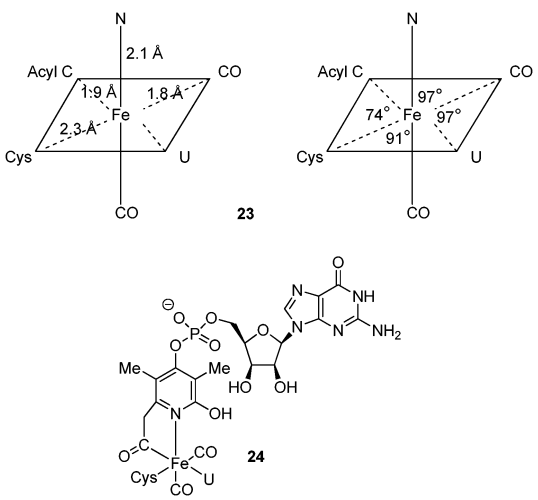

Fig. 12 Revised crystal structure for "wild-type" Hmd.

Based on all of the above studies it appears likely that the iron in the active site of the [Fe]-hydrogenase is ligated by the ring nitrogen and acyl carbon of the pyridinol ligand, two intrinsic CO molecules, the sulfur of Cys176 and an unknown ligand U, affording an overall complex represented in different styles as **23** or **24**. It is thought that both $CH{\equiv}H_4MPT^+$ **1** and H_2 can enter the active site *via* a channel in the protein and that the action of the cationic substrate **1** and Lewis acidic Fe heterolytically cleave molecular hydrogen, though the exact mechanism is not known. $CH{\equiv}H_4MPT^+$ **1** can be orientated close to the iron centre and even interact with the ligands of the iron, but it is not thought to bond directly to the iron centre during the reaction, although it has not been fully discounted. Mössbauer studies[40] on the iron centre showed no significant change on addition of **1** to the enzyme, however, no significant changes were observed on the addition of H_2.

With the structure of [Fe]-hydrogenase determined and the geometry of the active site elucidated, the next stage in development will be obtaining a plausible mechanism for the reaction of $CH{\equiv}H_4MPT^+$ **1** with molecular hydrogen.

Computational modelling involving the iron complex

Since reporting of the crystal structure of Hmd, it was entirely as expected that much work would be conducted in order to try and understand the mechanism of reaction of this unusual enzyme. As a result of this, a variety of mechanistic studies have been reported in an attempt to explain its unusual reactivity. This section examines these literature reports.

First reported crystal structure

Yang and Hall[45] reported a trigger mechanism for the reaction of Hmd using density functional theory calculations. They used complex **25** (Scheme 9) as a model for the then-determined active-site **20**. Several differences in model **25** to the active site are apparent. The hydroxyl group in the model had been moved from the 2-position of the pyridine in the real group to the 3-position in this model in order to prevent it from strongly interacting with the sulfur or CO groups bound to the iron. Furthermore the replacement of the phosphate ester at the 4-position of the pyridine ring by a pyridinol hydroxyl group is a significant deviation from the structure of the true cofactor (unless the true cofactor were to undergo phosphate ester hydrolysis as part of the catalytic cycle). Another significant proposal was inclusion of an oxygen bound to the iron in place of the unknown ligand, the oxygen coming from the

View Online

Downloaded by Ludwig Maximilians Universitaet Muenchen on 28 June 2011
Published on 01 March 2011 on http://pubs.rsc.org | doi:10.1039/C0CS00150C

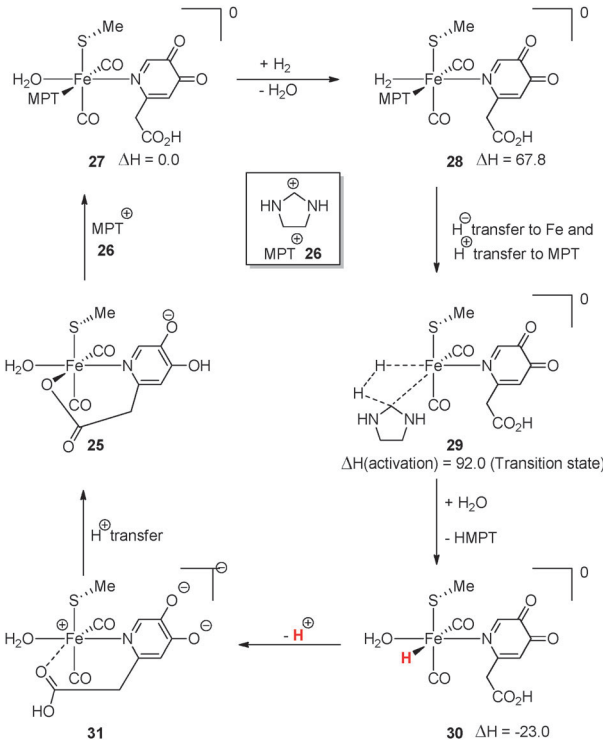

Scheme 9 Proposed mechanism, based on computation, of H_2 splitting by model **25**.[45] Energies are in kJ mol^{-1}. The representation of localised charges in **25** and **31** represents our (MJC, JAM) interpretation of the published scheme to allow easy visualization of reactivity. We thank Prof. Hall for helpful discussions.

carboxylate chain on the pyridone ring. The calculated IR values of the CO ligands in model **25** were 1957 and 2014 cm^{-1} (*cf.* 1944 and 2011 cm^{-1} in Hmd).[45]

The proposed mechanism is shown in Scheme 9. The conversion of complex **25** where an anionic carboxylate is bound to iron into complex **27** where MPT$^+$ **26** has bound to iron, involves the intramolecular transfer of two electrons from the pyridine ring to the iron, thereby inverting polarity at the iron and allowing it to attack the MPT$^+$ cation. The conversion of **28** to **29** involves formal proton transfer to the MPT carbon and hydride transfer to the iron atom. The conversion of **30** to **31** reverses the previous intramolecular two-electron transfer, leaving the iron polarized to accept the carboxyl group as a ligand, prior to proton transfer. In the absence of MPT$^+$ **26**, the splitting of H_2 was calculated with a barrier of 292 kJ mol^{-1}. In the presence of MPT$^+$ **26**, the activation barrier decreased to 92.0 kJ mol^{-1}. The authors stated that the exchange of H_2/H^+ in the mechanism is strongly dependent on MPT$^+$ **26** being present. Without it, H_2 splitting and the exchange of the proton with the protons of water will not occur. They stated that MPT$^+$ **26** or H_2 could arrive in any order at the active site, but that both must be present for the reaction to occur.

Most recent crystal structure models

With the reporting of a recalculated crystal structure[19] of the active-site of the [Fe]-hydrogenase, further proposed mechanisms and active-site models have been reported in the

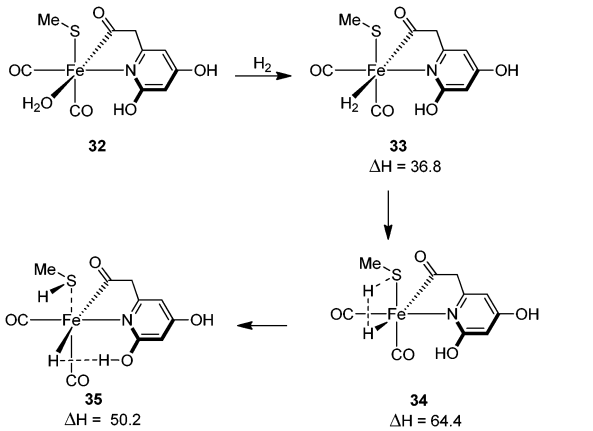

Scheme 10 Splitting of H_2 using computational model **32**.[48] Energies in kJ mol^{-1}.

literature. Yang and Hall[48] once again reported a trigger mechanism for the newly re-determined active-site based on model **32** (Scheme 10).

The authors proposed that complex **35** represents the cofactor within the resting state of the enzyme. Evidence for this was from the calculated vibrational frequencies of the *cis* CO units at 2007 and 1949 cm^{-1} closely resembling those of the wild-type Hmd. Also, upon addition of H_2, the Mössbauer spectrum of the iron in Hmd does not change significantly.[40] The authors proposed that complex **35** could be formed without significant alteration to the IR spectrum of Hmd. Complex **35** reacts with Ph–MPT$^+$ **41** undergoing hydride abstraction through transition state **36** (65.3 kJ mol^{-1}) to intermediate **37** (47.3 kJ mol^{-1}) (Scheme 11). Ph–HMPT then detaches from the complex to be replaced by H_2, resulting in formation of more stable complex **38**. Proton loss from **38** could then occur from Cys176 (to give **40**, 8.8 kJ mol^{-1}) or from the pyridinol ligand (to give **39**, 0.4 kJ mol^{-1}). This is where the observed H_2O/H^+ exchange catalysed by Hmd and **1**/**2** occurs. Subsequent H_2 cleavage occurs in **39** or **40** to give complex **35** and the catalytic cycle continues.

The authors stated that the model showed that the sulfur of Cys176 and the pyridine hydroxyl group were essential for the reaction to proceed, aiding in the splitting of H_2. It was also stated that in the absence of Ph–MPT$^+$ **41**, no H_2O/H^+ exchange (or similarly D_2O/H^+ exchange) would occur as the calculated deprotonation energies were too high (42–84 kJ mol^{-1}). The arrival of Ph–MPT$^+$ **41** triggers a breaking of the strong Fe–H–H–O bond in **35**, allowing the transfer of hydride to occur with an energy barrier of 65.3 kJ mol^{-1} (excluding the energy of H_2 splitting as shown in Scheme 10).

The calculated deprotonation energies are shown in Table 1. As can be seen, the exothermic deprotonations occur in complexes **37** and **38**, which occur after the reaction with Ph–MPT$^+$ **41**. These calculations are consistent with the observed reactivity of Hmd, where exchange was observed only in the presence of Hmd and CH$\equiv$H$_4$MPT$^+$ **1**/CH$_2$=H$_4$MPT **2**. However, it is unusual that the deprotonation of the sulfur of MeSH in complex **35** is calculated as being so endothermic (105 kJ mol^{-1}). If complexed to the iron centre, a species such

 This journal is © The Royal Society of Chemistry 2011

View Online

Downloaded by Ludwig Maximilians Universitaet Muenchen on 28 June 2011
Published on 01 March 2011 on http://pubs.rsc.org | doi:10.1039/C0CS00150C

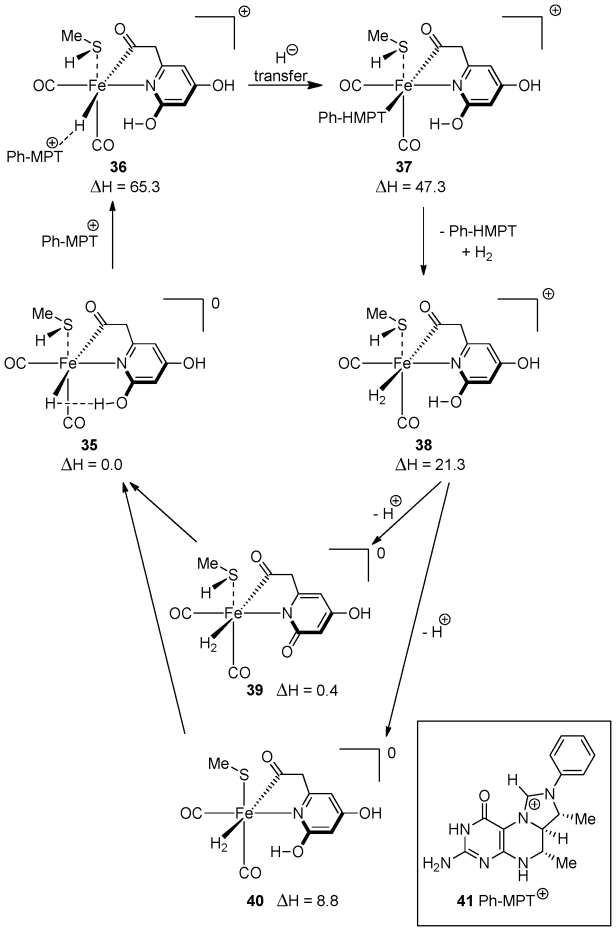

Scheme 11 Catalytic mechanism of reaction of Ph–MPT$^+$ **41** with H_2.[48] Energies in kJ mol^{-1}.

Table 1 Calculated deprotonation energies of various complexes (Schemes 10 and 11)

Deprotonation site	ΔG/kJ mol^{-1}
Pyridinol O in **33**	84
Pyridinol O in **35**	163
Cys176 S in **35**	105
Cys176 S in **37**	−38
Pyridinol O in **38**	−21
Thiol S in **38**	−13
Thiol S in **39**	96

as R_2SH^+ would be expected to be easily deprotonated. If this was to occur, it would allow H^+/H_2O exchange in the absence of $CH{\equiv}H_4MPT^+$ **1**/$CH_2{=}H_4MPT$ **2**, a reactivity that is not observed in Hmd.

A further development was reported by Shima *et al.*[49] They reported the crystal structure of a binary complex of Cys176–Ala-mutated [Fe]-hydrogenase with $CH_2{=}H_4MPT$ **2** at 2.15 Å resolution. The results showed that $CH_2{=}H_4MPT$ **2** fitted into the active-site cleft of [Fe]-hydrogenase (Fig. 14). In the crystal structure obtained, the N^5 and N^{10} of the imidazolidine ring were found to be planar, rather than in the non-planar active form of the substrate. The authors stated that the non-planar active form could be induced by rotation of the phenyl ring adjacent to the imidazolidine ring that could

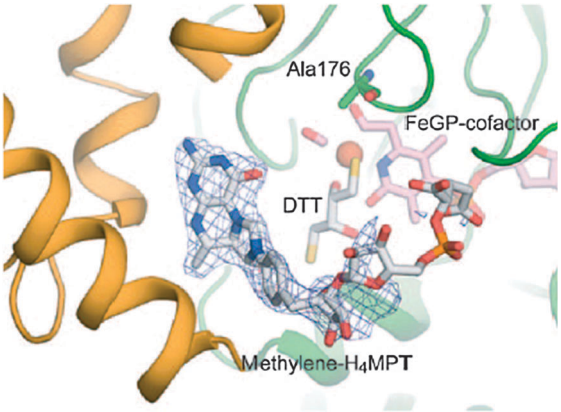

Fig. 14 Active-site crystal structure of Cys176-Ala-mutated [Fe]-hydrogenase. Ref. 49. Copyright Wiley-VCH Verlag GmbH & Co. KGaA. Reproduced with permission.

occur in the closed form of the enzyme. The authors stated that in the open-form of the enzyme crystallised, no carboxy group was present to protonate one of the nitrogens of $CH{\equiv}H_4MPT^+$ **1**. This protonation would be necessary for the superelectrophilic activation mechanism proposed previously (Schemes 6 and 7). In the open form of the enzyme crystallised, it was found that the C_{14a} of $CH_2{=}H_4MPT$ **2** and iron of the active-site were separated by a distance of 9.3 Å, too far for hydride transfer.

Shima *et al.*[49] modelled the closed form of the enzyme with $CH_2{=}H_4MPT$ **2** present (Fig. 15). In this model, the distance between C_{14a} of $CH_2{=}H_4MPT$ **2** and iron of the active-site decreased to only 3 Å. The model showed that the C_{14a} of $CH_2{=}H_4MPT$ **2** lay *trans* to the acyl carbon of the pyridinol ligand **31**, suggesting that the site of H_2 activation was in the position *trans* to the acyl carbon inhabited by the unknown ligand (U in **24**, Fig. 12).

Based on the crystal structure, they proposed a catalytic mechanism based on an open/closed conformational transition (Scheme 12). The catalytic cycle is initiated by binding of $CH{\equiv}H_4MPT^+$ **1** to the open form of the enzyme (**42**, Scheme 12), causing the closure of the cleft to give the closed conformation (**43**, Scheme 12). This closure could induce conformational changes in $CH{\equiv}H_4MPT^+$ **1**, enhancing its carbocationic character. H_2 is then captured at the site of the unknown ligand, the proposed site of H_2-activation, binding side-on to the iron (**44**, Scheme 12). The H_2 molecule becomes polarised and can be heterolytically cleaved by the adjacent carbocation (C_{14a} of $CH{\equiv}H_4MPT^+$ **1**). The hydride is accepted by $CH{\equiv}H_4MPT^+$ **1** and the resulting proton is proposed to be taken by a base (either the Cys176 thiol or pyridinol oxygen). The results in formation of $CH_2{=}H_4MPT$ **2** and a proton, which can undergo the exchange reactions detailed above.

It was stated that no carboxy group was present to protonate one of the nitrogens of $CH{\equiv}H_4MPT^+$ **1**, however, in the modelled active-site **43**, it was also stated that the hydroxyl group of the pyridinol ring could interact with the N^{10} of $CH{\equiv}H_4MPT^+$ **1**, which the authors proposed could modify the properties of the pyridinol. The possibility of such

View Online

Downloaded by Ludwig Maximilians Universitaet Muenchen on 28 June 2011
Published on 01 March 2011 on http://pubs.rsc.org | doi:10.1039/C0CS00150C

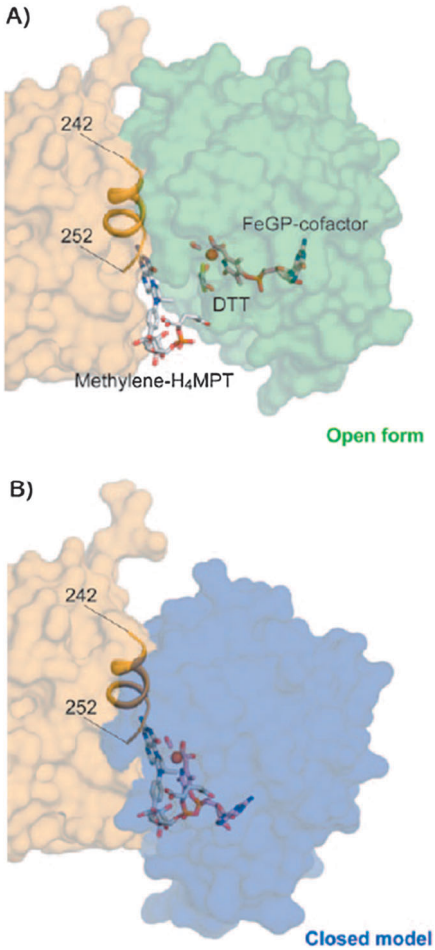

Fig. 15 (A) Crystal structure representation of Cys176-Ala-mutated [Fe]-hydrogenase and $CH_2{=}H_4MPT$ **2**. B) Modelled closed-form of enzyme with $CH_2{=}H_4MPT$ **2** present. Ref. 49. Copyright Wiley-VCH Verlag GmbH & Co. KGaA. Reproduced with permission.

an interaction enabling the superelectrophilic activation has previously been discussed.

Chemical models of the cofactor and substrate

Modelling of the FeGP cofactor is being undertaken by many groups. Royer *et al.*[50] reported the synthesis of iridium complex **46** as a model for the (then reported) active-site of Hmd. This model showed binding to the metal centre by the ring nitrogen in the pyridinol form (as shown by X-ray crystallography). In terms of hydrogenase-related activity, model **46** was able to dehydrogenate 1-phenylethanol **47** catalytically to acetophenone **48** (Scheme 13). In relation to the more recent proposals that the FeGP cofactor contains an iron acyl (structure **22** in Fig. 10) linkage, and noting also the presence of the cysteine thiolate ligand, Royer, Rauchfuss and Gray[51,52] used oxidative addition of iron to thioester **49** to generate an unstable compound that they assigned as their target, **50**; in the presence of cyanide, the unstable compound was transformed into stable cyanide complex **51** (Scheme 14).

Hu *et al.* prepared[53] model **52**, incorporating a 2-pyridone ligand, while Popescu, Darensbourg *et al.*, published[54] the

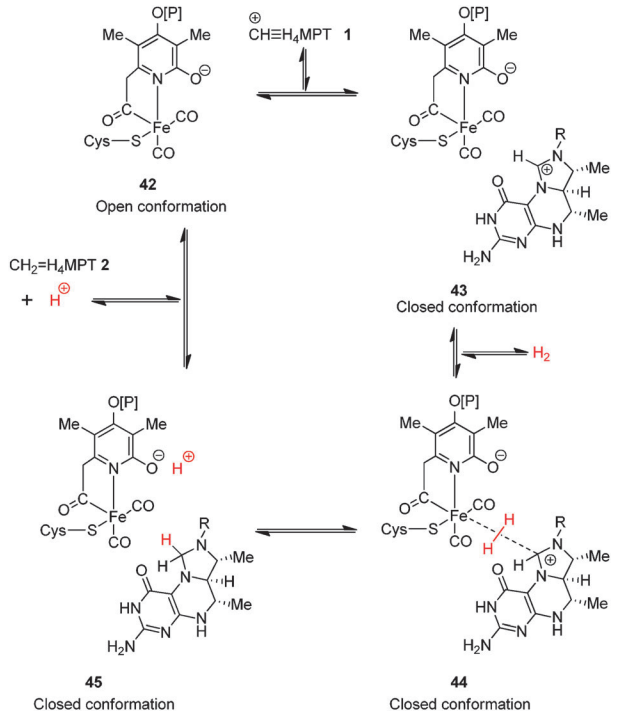

Scheme 12 Proposed catalytic mechanism for open/closed conformational transition.[49]

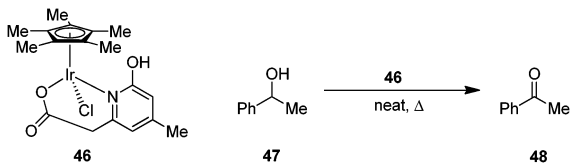

Scheme 13 Hmd active site model **46**.

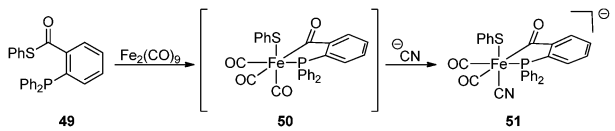

Scheme 14 Oxidative addition with a thioester.

analogous complex **53** with a pyridine-2-thione in place of the 2-pyridone shortly afterwards. More recently, Hu's group prepared[55] complexes **54**. With a pyridine, a thiolate, a *cis*-dicarbonyl and an acyl all complexed to iron(II), this complex has a number of similarities to the FeGP cofactor.

The group of Pickett has also been active in preparation of model iron complexes. Their earlier work[41] had prepared the *cis*-dicarbonyliron complex **55**, which had been useful in their study assigning iron(II) as the metal oxidation state in FeGP. In 2010, Pickett *et al.* prepared the advanced analogue **56**,[56] giving CO stretches in the IR spectrum at 2026 and 1958 cm^{-1} (compared to 2031 and 1972 cm^{-1} in the FeGP complex). Also in 2010, the Hu group reported the preparation and properties of sophisticated iron acyl complexes **57** (Fig. 16).[57,58]

The organic substrates for the transformations of this enzyme $CH{\equiv}H_4MPT^+$ **1** and $CH_2{=}H_4MPT$ **2** are known, but proposals on how these substrates may be activated

 This journal is © The Royal Society of Chemistry 2011

View Online

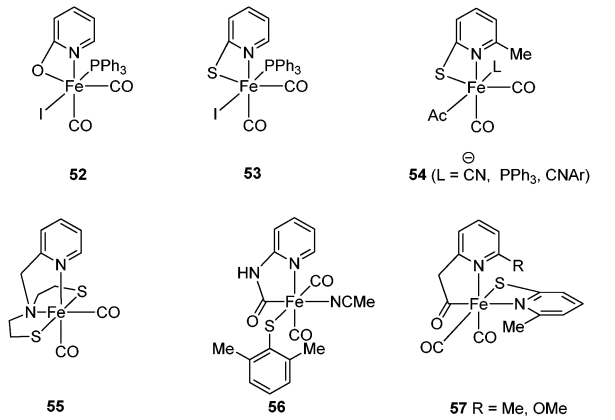

Fig. 16 Synthesised models of the iron complex in the [Fe]-hydrogenase.

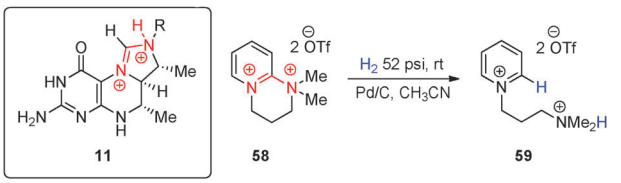

Scheme 15 Amidine dication **58**, reacts readily with H_2 at the amidine carbon.

electronically or stereoelectronically in the active site of the [Fe]-hydrogenase have been prominent in the development of our understanding of this enzyme. As mentioned above, Berkessel and Thauer proposed that to receive a formal hydride ion, activation of **2** by pyramidalisation of the imidazolinium nitrogens by protonation (or through hydrogen-bonding) would convert it into a superelectrophilic amidine species **11** or **12** (Scheme 6). Until recently, such highly activated amidine dications were unknown as isolated species, but Corr *et al.*[59,60] recently announced synthetic routes to these species (Scheme 15). Unsurprisingly, such compounds are highly electrophilic and react readily with hydrogen gas. Thus disalt **58** was converted into pyridinium salt **59** under mild conditions. Product pyridinium salt **59** was inert under these conditions showing the hightened reactivity of the amidine disalt **58**. Although highly reactive, a catalyst was still needed. In this case, the addition of hydrogen may require that the aromaticity of the pyridinium ring in **58** is temporarily disrupted, and hence it will be of interest to test the reactivity of closer models to the activated forms of $CH{\equiv}H_4MPT^+$ **1**, in its conversion to $CH_2{=}H_4MPT$ **2**, if such model compounds can be prepared.

Summary and outlook

This review shows that our understanding of the [Fe]-hydrogenase enzyme, first reported 20 years ago, is now moving forward at a prodigious rate. Early mechanistic work provided crucial information on the complexity of the exchange reactions between dihydrogen and water, as well as the need for activation of the organic substrate **1** and dihydrogen for the conversion into reduced substrate **2**.

The key subsequent finding that an iron complex with a unique pyridine ligand is at the heart of the enzyme, together with the provision of the first crystal structure allowed further ideas to be developed about the possible pathway of the reaction and computational studies to be published that considered all intermediates in a putative catalytic cycle. The subsequent refinement, arising from further X-ray crystallography studies, to our knowledge of the nature of the bonding within the iron complex, and the realization that a unique iron–acyl is present, have prompted synthesis of model complexes that are now reaching a new level of sophistication. Future challenges will be to produce a working model in which an appropriate iron complex, dihydrogen and an organic substrate can, with due activation, mimic the reaction in the enzyme.

If lessons can be learned from the mechanisms of action of the hydrogenase enzymes that use accessible metals, iron and nickel, to harness the reductive power of H_2 economically, this could prove of great benefit to our future. Of course, other important and related lessons can be learned by a study of cooperative microorganisms that manage methane production in nature, such as the facile generation and transport of H_2 as shown in Scheme 1 for providing the hydrogen in new, efficient and convenient ways.

Notes and references

1 R. K. Thauer, A.-K. Kaster, M. Goenrich, M. Schick, T. Hiromoto and S. Shima, *Annu. Rev. Biochem.*, 2010, **79**, 507–536.
2 B. Schink, *Microbiol. Mol. Biol. Rev.*, 1997, **61**, 262–280.
3 H. A. Barker, *Antonie van Leeuwenhoek*, 1940, **6**, 201–220.
4 M. P. Bryant, E. A. Wolin, M. J. Wolin and R. S. Wolfe, *Arch. Mikrobiol.*, 1967, **59**, 20–31.
5 D. M. Heinekey, *J. Organomet. Chem.*, 2009, **694**, 2671–2680.
6 J. C. Fontecilla-Camps, A. Volbeda, C. Cavazza and Y. Nicolet, *Chem. Rev.*, 2007, **107**, 4273–4303.
7 P. M. Vignais and B. Billoud, *Chem. Rev.*, 2007, **107**, 4206–4272.
8 S. Canaguier, V. Artero and M. Fontecave, *Dalton Trans.*, 2008, 315–325.
9 C. Tard and C. J. Pickett, *Chem. Rev.*, 2009, **109**, 2245–2274.
10 E. Garcin, X. Vernede, E. C. Hathikian, A. Volbeda, M. Frey and J. C. Fontecilla-Camps, *Structure (London)*, 1999, **7**, 557–566.
11 C. Zirngibl, R. Hedderich and R. K. Thauer, *FEBS Lett.*, 1990, **261**, 112–116.
12 C. Zirngibl, W. Van Dongen, B. Schwörer, R. Von Bünau, M. Richter, A. Klein and R. K. Thauer, *Eur. J. Biochem.*, 1992, **208**, 511–520.
13 J. Schleucher, C. Griesinger, B. Schwörer and R. K. Thauer, *Biochemistry*, 1994, **33**, 3986–3993.
14 This enzyme performs an analogous task to F420-dependent methylenetetrahydromethanopterin dehydrogenase, which uses the reduced form of cofactor F420 in place of H_2 as the reducing entity. See K. Ceh, U. Demmer, E. Warkentin, J. Moll, R. K. Thauer, S. Shima and U. Ermler, *Biochemistry*, 2009, **48**, 10098–10105.
15 R. K. Thauer, A. R. Klein and G. C. Hartmann, *Chem. Rev.*, 1996, **96**, 3031–3042.
16 A. Berkessel and R. K. Thauer, *Angew. Chem., Int. Ed. Engl.*, 1995, **34**, 2247–2250.
17 E. J. Lyon, S. Shima, G. Buurman, S. Chowdhuri, A. Batschauer, K. Steinbach and R. K. Thauer, *Eur. J. Biochem.*, 2004, **271**, 195–204.
18 S. Shima, O. Pilak, S. Vogt, M. Schick, M. S. Stagni, W. Meyer-Klaucke, E. Warkentin, R. K. Thauer and U. Ermler, *Science*, 2008, **321**, 572–575.

Downloaded by Ludwig Maximilians Universitaet Muenchen on 28 June 2011
Published on 01 March 2011 on http://pubs.rsc.org | doi:10.1039/C0CS00150C

View Online

19 T. Hiromoto, K. Ataka, O. Pilak, S. Vogt, M. S. Stagni, W. Meyer-Klaucke, E. Warkentin, R. K. Thauer, S. Shima and U. Ermler, *FEBS Lett*., 2009, **583**, 585–590.
20 R. von Bünau, C. Zirngibl, R. K. Thauer and A. Klein, *Eur. J. Biochem*., 1991, **202**, 1205–1208.
21 S. P. J. Albracht, in *The Molecular Basis of Bacterial Metabolism*, ed. G. Hauska, R. K Thauer, Springer, Berlin, 1990, pp. 40–51.
22 B. Schwörer, V. M. Fernandez, C. Zirngibl and R. K. Thauer, *Eur. J. Biochem*., 1993, **212**, 255–261.
23 R. Breslow, *J. Am. Chem. Soc*., 1957, **79**, 1762–1763.
24 M. Scholl, S. Ding, C. W. Lee and R. H. Grubbs, *Org. Lett*., 1999, **1**, 953–956.
25 G. Buurman, S. Shima and R. K. Thauer, *FEBS Lett*., 2000, **485**, 200–204.
26 G. A. Olah, A. Germain, H. C. Lin and D. A. Forsyth, *J. Am. Chem. Soc*., 1975, **97**, 2928–2929.
27 G. A. Olah, G. K. Surya Parakash and J. Sommer, *Superacids*, Wiley, New York, 1985.
28 G. A. Olah, in *The Chemistry of Alkanes and Cycloalkanes*, ed. S. Patai, Wiley, New York, 1992, pp. 609–652.
29 G. A. Olah and D. A. Klumpp, *Superelectrophiles and Their Chemistry*, Wiley-Interscience, 2007.
30 A. R. Klein, G. C. Hartmann and R. K. Thauer, *Eur. J. Biochem*., 1995, **233**, 372–376.
31 A. R. Klein, V. M. Fernandez and R. K. Thauer, *FEBS Lett*., 1995, **368**, 203–206.
32 J. Cioslowski and G. Bhe, *Angew. Chem., Int. Ed. Engl*., 1997, **36**, 107–109.
33 J. H. Teles, S. Brode and A. Berkessel, *J. Am. Chem. Soc*., 1998, **120**, 1345–1346.
34 A. P. Scott, B. T. Golding and L. Radom, *New J. Chem*., 1998, **22**, 1171–1173.
35 A. Berkessel, *Curr. Opin. Chem. Biol*., 2001, **5**, 486–490.
36 E. J. Lyon, S. Shima, G. Buurman, S. Chowdhuri, A. Batschauer, K. Steinbach and R. K. Thauer, *Eur. J. Biochem*., 2003, **271**, 195–204.
37 E. J. Lyon, S. Shima, R. Boecher, R. K. Thauer, F.-W. Grevels, E. Bill, W. Roseboom and S. P. J. Albracht, *J. Am. Chem. Soc*., 2004, **126**, 14239–14248.
38 S. Shima, E. J. Lyon, M. Sordel-Klippert, M. Kauβ, J. Kahnt, R. K. Thauer, K. Steinbach, X. Xie, L. Verdier and C. Griesinger, *Angew. Chem., Int. Ed*., 2004, **43**, 2547–2551.
39 S. A. Goldfield and K. N. Raymond, *Inorg. Chem*., 1974, **13**, 770–775.
40 S. Shima, E. J. Lyon, R. K. Thauer, B. Mienert and E. Bill, *J. Am. Chem. Soc*., 2005, **127**, 10430–10435.
41 X. Wang, Z. Li, X. Zeng, Q. Luo, D. J. Evans, C. J. Pickett and X. Liu, *Chem. Commun*., 2008, 3555–3557.
42 M. Salomone-Stagni, F. Stellato, C. M. Whaley, S. Vogt, S. Morante, S. Shima, T. R. Rauchfuss and W. Meyer-Klaucke, *Dalton Trans*., 2010, **39**, 3057–3064.
43 O. Pilak, B. Mamat, S. Vogt, C. H. Hagemeier, R. K. Thauer, S. Shima, C. Vonrhein, E. Warkentin and U. Ermler, *J. Mol. Biol*., 2006, **358**, 798–809.
44 P. Acharya, M. Goenrich, C. H. Hagemeier, U. Semmer, J. A. Vorholt, R. K. Thauer and U. Ermler, *J. Biol.Chem*., 2005, **280**, 13712–13719.
45 X. Yang and M. B. Hall, *J. Am. Chem. Soc*., 2008, **130**, 14036–14037.
46 The Fe–GP cofactor in the active enzyme shows CO stretching frequencies similar to η^5-(cyclopentadienyl)dicarbonylacyliron complexes in organic solvents or in the dried state. S. T. Belt, D. W. Ryba and P. C. Ford, *J. Am. Chem. Soc*., 1991, **113**, 9524–9528.
47 E. Baranowska, W. Danikiewicz, Z. Pakulski and A. Zamojski, *J. Mass Spectrom*., 1995, **30**, 158–162.
48 X. Yang and M. B. Hall, *J. Am. Chem. Soc*., 2009, **131**, 10901–10908.
49 T. Hiromoto, E. Warkentin, J. Moll, U. Ermler and S. Shima, *Angew. Chem., Int. Ed*., 2009, **48**, 6457–6460.
50 A. M. Royer, T. B. Rauchfuss and S. R. Wilson, *Inorg. Chem*., 2008, **47**, 395–397.
51 A. M. Royer, T. B. Rauchfuss and D. L. Gray, *Organometallics*, 2009, **28**, 3618–3620.
52 A. M. Royer, M. Salomone-Stagni, T. B. Rauchfuss and W. Meyer-Klaucke, *J. Am. Chem. Soc*., 2010, **132**, 16997–17003.
53 B. V. Obrist, D. Chen, A. Ahrens, V. Schünemann, R. Scopelliti and X. Hu, *Inorg. Chem*., 2009, **48**, 3514–3516.
54 B. Li, T. Liu, C. V. Popescu, A. Bilko and M. Y. Darensbourg, *Inorg. Chem*., 2009, **48**, 11283–11289.
55 D. Chen, R. Scopelliti and X. Hu, *J. Am. Chem. Soc*., 2010, **132**, 928–929.
56 P. J. Turrell, J. A. Wright, J. M. T. Peck, V. S. Oganesyan and C. J. Pickett, *Angew. Chem., Int. Ed*., 2010, **49**, 7508–7511.
57 D. Chen, R. Scopelliti and X. Hu, *Angew. Chem., Int. Ed*., 2010, **49**, 7512–7515.
58 For a recent simpler 2-methoxypyridine complex see S. Tanino, Y. Ohki and K. Tatsumi, *Chem.–Asian J*., 2010, **5**, 1962–1964.
59 M. J. Corr, K. F. Gibson, A. R. Kennedy and J. A. Murphy, *J. Am. Chem. Soc*., 2009, **131**, 9174–9175.
60 M. J. Corr, M. Roydhouse, K. F. Gibson, S. Zhou, A. R. Kennedy and J. A. Murphy, *J. Am. Chem. Soc*., 2009, **131**, 17980–17985.
61 J. A. Wright, P. J. Turrell and C. J. Pickett, *Organometallics*, 2010, **29**, 6146–6156.
62 S. Shima and U. Ermler, *Eur. J. Inorg. Chem*., DOI: 10.1002/ejic.201000955 published on line 2010.

Downloaded by Ludwig Maximilians Universitaet Muenchen on 28 June 2011
Published on 01 March 2011 on http://pubs.rsc.org | doi:10.1039/C0CS00150C

 This journal is © The Royal Society of Chemistry 2011